

**SCHOOL OF MATERIALS AND MINERAL RESOURCES ENGINEERING
UNIVERSITI SAINS MALAYSIA**

**EFFECT OF ZnO SEED LAYER ON THE GROWTH OF ZnO NANORODS
VIA SOLUTION PRECIPITATION METHOD**

By

NIK ANIS HAFIZA BT NIK JUSOH

Supervisor: Assoc. Prof. Ir. Dr. Pung Swee Yong

Dissertation submitted in partial fulfillment
of the requirements for the Degree of Bachelor Engineering with Honours
(Materials Engineering)

Universiti Sains Malaysia

JUNE 2018

DECLARATION

I hereby declare that I have conducted, completed the research work and written the dissertation entitles “**Effect of ZnO seed layer on the growth of ZnO nanorods via solution precipitation method**”. I also declared that it has not been previously submitted for the award for any degree or diploma or other similar title of this for any other examining body or University.

Name of Student : Nik Anis Hafiza bt Nik Jusoh

Signature:

Date :

Witnessed by

Supervisor : Assoc. Prof. Ir. Dr. Pung Swee Yong

Signature:

Date :

ACKNOWLEDGEMENTS

First and foremost, praise to Allah SWT, the Almighty for His blessing throughout my final year project and for giving me the strength that I needed in order to complete this project.

I would like to express my most sincere gratitude to my supervisor Assoc. Prof. Ir. Dr. Pung Swee Yong for the continuous support on my final year project, for his patience, motivation, enthusiasm, and immense knowledge. His guidance has helped me a lot throughout this project as well as for providing necessary information regarding the project and for his support in completing the project. I could not imagined having a better advisor and mentor for my final year project.

Next, I would like to extend my gratitude to the postgraduate students who always helped me during my laboratory works, which are May Zin Toe, Mrs Qurratu Aini and Lee Anh Thi for their encouragement, insightful comments and valuable guidance extended to me. I gained a lot of new knowledge regarding the research and laboratory works all thanks to them. Besides that, I would like to express my appreciation to the technical staffs which are En Zul, En Khairi, En Rashid, En Azrul, En Zaini, En Azam, En Syafiq and Pn Haslina for their great help in providing me with all the necessary facilities, equipments and recommendations in solving problem throughout the project.

I also wish to express my deepest thanks to my family, especially my parents for their unwavering support and encouragement during all the good and hard times for me to finish this project. I also place on records, my sense of gratitude to one and all, who directly and indirectly, have lent their hands in this endeavor. It would not have been possible without the kind support and help of many individuals and organizations.

TABLE OF CONTENTS

Contents	Page
DECLARATION	ii
ACKNOWLEDGEMENTS	iii
LIST OF FIGURES	vi
LIST OF TABLES	xii
LIST OF ABBREVIATIONS.....	xiii
LIST OF SYMBOLS	xiv
ABSTRAK.....	xv
ABSTRACT.....	xvi
CHAPTER 1 INTRODUCTION	1
1.1 Introduction	1
1.2 Problem statement.....	2
1.3 Research objectives	5
1.4 Project overview.....	5
1.5 Thesis outline	8
CHAPTER 2 LITERATURE REVIEW	9
2.0 History and background	9
2.1 ZnO properties	9
2.2 Synthesis methods of ZnO nanostructures	13
2.2.1 Solution routes	13
2.2.1.1 Sol-gel method	13
2.2.1.2 Hydrothermal method	14
2.2.1.3 Solution Precipitation method.....	15
2.2.1.4 Factors that affect ZnO nanorods growth using solution route.....	17
2.2.2 Vapor routes.....	22
2.2.2.1 Chemical Vapor Deposition (CVD) method.....	22
2.2.2.2 Physical Vapor Deposition (PVD) method.....	25
.....	26
2.2.2.3 Atomic Layer Deposition (ALD) method	26
2.3 Synthesis of aligned ZnO nanorods	27
2.3.1 Use of substrates with small lattice mismatch with ZnO	27
2.3.2 Use of highly (002) oriented ZnO seeds layer.....	31
2.4 Applications of ZnO nanomaterials	33

CHAPTER 3 MATERIALS AND METHODOLOGY	38
3.1 Introduction	38
3.2 Raw materials and chemicals	38
3.3 Experimental procedure	38
3.3.1 Deposition of ZnO seed layers on Si substrates	41
3.3.2 Growth of ZnO nanorods via solution precipitation method	42
3.3.1.1 Effect of rotational speed (rpm) of spin coater	44
3.3.1.2 Effect of coating cycles of ZnO seed layer	44
3.3.1.3 Effect of annealing temperature of ZnO seed layer	45
3.4 Characterization of ZnO seed layers and ZnO Nanorods on Si substrates	46
3.4.1 Field Emission Scanning Electron Microscopy (FESEM)	46
3.4.2 X-Ray Diffraction (XRD)	48
3.4.3 UV-Visible spectroscopy	49
3.4.4 Wetting Contact Angle (WCA)	50
CHAPTER 4 RESULTS AND DISCUSSIONS	52
4.1 Introduction	52
4.2 Synthesis and characterization of ZnO nanorods on Si substrate	52
4.2.1 Without ZnO seed layer (bare Si substrate)	52
4.2.2 With ZnO seed layer	54
4.2.2.1 Effect of rotational speed (rpm) of spin coater	54
4.2.2.2 Effect of coating cycles of ZnO seed layer	57
4.2.2.3 Effect of annealing temperature of ZnO seed layer	60
4.3 UV-Visible Spectroscopy	64
4.4 Wetting Contact Angle (WCA)	65
4.5 Growth mechanism of ZnO nanorods	67
4.5.1 Growth of ZnO nanorods	67
4.5.1.1 On bare Si substrate	67
4.5.1.2 On (002) oriented ZnO seed layer pre-deposited on Si substrate	69
CHAPTER 5 CONCLUSIONS AND RECOMMENDATIONS	71
5.1 Conclusions	71
5.2 Future works	72
REFERENCES	73

LIST OF FIGURES

Figure 1.1: ZnO nanorods based (a) LED (Choi et al., 2010), (b) FET (Tsai <i>et al.</i> , 2011) and (c) solar cell (Hames <i>et al.</i> , 2010).....	3
Figure 1.2: Randomly aligned ZnO nanorods grown on silicon substrate via sol-gel technique (Ibupoto et al., 2013)	4
Figure 1.3: Process flow of synthesis and growth of ZnO nanorods on Si substrate.....	7
Figure 2.1: Hexagonal wurtzite structure model of ZnO (Vaseem, Umar and Hahn, 2010)	11
Figure 2.2: ZnO nanostructures (a) nanobelts, (b) nanorings, (c) nanowires and (d) nanocages (Wang, 2004)	12
Figure 2.3: Growth morphologies of 1D ZnO nanostructures and corresponding facets (Wang, 2004)	12
Figure 2.4: ZnO nanorods synthesized by sol-gel method (Kashif et al., 2013)	14
Figure 2.5: FESEM image of ZnO nanorods synthesized by hydrothermal method (Ridhuan et al., 2012)	15
Figure 2.6: SEM micrographs of ZnO nanoparticles synthesized by solution precipitation method and synthesized at different annealing temperatures (a) as-obtained precursor, (b) 250°C, (c) 350°C, (d) 450°C and © 550°C (Raoufi, 2013)	16
Figure 2.7: SEM image of ZnO nanorods by varying stirring solutions (a) 1hr, (b) 3hrs, (c) 5hrs and (d) 15hrs respectively (Alnoor et al., 2015)	17

Figure 2.8: FESEM images of ZnO nanorods synthesized at different precursor concentrations (1 Mm to 9 Mm) respectively (Mustafa et al., 2017)	19
Figure 2.9: SEM images of ZnO nanostructures on Si substrates grown with different aqueous solutions at (a) pH value of 1.8, (b) pH value of 4.6, (c) pH value of 6.6, (d) pH value of 9.1.....	20
Figure 2.10: Cross-sectional SEM images of ZnO nanorods at different growth times; (a) 1hr, (b) 3 hrs, (c) 6 hrs, and (d) 10 hrs. The inset shows the corresponding top view of SEM images (Amin et al., 2011)	21
Figure 2.11: Schematic diagram of CVD process (Kim, Kim and Kim, 2017)	23
Figure 2.12: ZnO nanorods synthesized by CVD method, (a) low magnification SEM image, (b) high magnification SEM image, and (c) top view of SEM image (Wang et al., 2004)	23
Figure 2.13: Room temperature photoluminescence (PL) emission spectra for ZnO nanoparticles at different annealing temperatures (Raoufi, 2013).....	24
Figure 2.14: SEM image of ZnO nanostructures synthesized by PVD method; (a) nanowires, and (b) nanosheets (Comini et al., 2010)	26
Figure 2.15: ZnO nanorods synthesized by ALD method (Thomas and Cui, 2012).....	27
Figure 2.16: SEM images of randomly aligned ZnO nanorods grown on (a) GaAs substrate (Zeng et al., 2010) and (b) ITO substrate (Gu et al., 2009).....	29

Figure 2.17: SEM images of aligned ZnO nanorods grown on GaN substrate, (a) low magnification side view image , (b) high magnification side view image, and (c) high magnification top view image (Wang et al., 2005).....	30
Figure 2.18: SEM images of ZnO nanorods on sapphire substrates with different seed layer thickness; (a) one seed layer, (b) three seed layer, (c) five seed layer, and (d) seven seed layer (Jia et al., 2013).....	30
Figure 2.19: XRD analysis on ZnO layers deposited on (100) Si substrate by different temperature using ALD technique (Pung, Choy and Hou, 2013).....	32
Figure 2.20: Deposition of highly (002) oriented ZnO layer on (100) Si substrate (Pung, Choy and Hou, 2013).....	32
Figure 2.21: Aligned ZnO nanorods grown on highly (002) oriented ZnO layer using CVD technique (Pung, Choy and Hou, 2013).....	33
Figure 2.22: ZnO nanostructures with different morphologies grown at various locations inside quartz tube. (a) EDX spectrum for Fig. 2.20 (a), (c) low magnification of grown ZnO nanorods inside quartz tube, (d) magnified image (Al-Ruqeishi et al., 2016).....	34
Figure 2.23: SEM images of ZnO nanorods with zinc acetate and HMTA solution at (a) 0.001M, (b) 0.01M, and (c) 0.1M (Kumar et al., 2015).....	35
Figure 2.24: Mechanism of photocatalytic reaction of semiconductor photocatalysts for organic pollutants removal (Binas et al., 2017).....	37
Figure 2.25: ZnO nanoparticles with various morphologies (a) rod-like, (b) needle-like, (c) needle-like, (d) rugby-like, and © flower-like demonstrated different photocatalytic performance under UV light irradiation (Xie et al., 2011).....	37

Figure 3.1: Overall process flow of synthesis of ZnO nanorods on Si substrate.....	40
Figure 3.2: Spin coater machine (a) spin coater setup, (b) Sample stage.....	42
Figure 3.3: Growth of ZnO nanorods by solution precipitation method.....	43
Figure 3.4: Temperature profile of annealing process.....	43
Figure 3.5: Process flow of deposition of ZnO seed layer to improve surface coverage of ZnO nanorods.....	45
Figure 3.6: Process flow of deposition of ZnO seed layer to improve alignment of ZnO nanorods.....	46
Figure 3.7: Schematic diagram of SEM working principle (Zhu et al., 2014).....	47
Figure 3.8: Schematic diagram of XRD analysis based on $\theta - 2\theta$ approach.....	49
Figure 3.9: Setup of sample for reflectance test using UV-Vis spectroscopy machine.....	50
Figure 3.10: Goniometer Rame Hart 260' machine for wetting contact angle measurement.....	51
Figure 4.1: XRD patterns of ZnO nanorods on Si substrate without ZnO seed layer...53	53
Figure 4.2: FESEM images of ZnO nanorods grown on bare Si substrate without ZnO seed layer.....	54
Figure 4.3: XRD patterns of ZnO nanorods grown ZnO seed layer prepared at various rotational speed of spin coater.....	56

Figure 4.4: FESEM images of ZnO nanorods grown on ZnO seed layers prepared at different rotational speed of spin coater (a) 0 rpm, (b) 1000 rpm, (c) 2000 rpm, (d) 2500 rpm, and (e) 3000 rpm.....	57
Figure 4.5: XRD patterns of ZnO nanorods grown on ZnO seed layers prepared at different coating cycles	58
Figure 4.6: FESEM images of ZnO nanorods grown on ZnO seed layers prepared at at different coating cycles (a) 0 cycles, (b) 3 cycles, (c) 5 cycles, (d) 7 cycles, (e) 9 cycles and (f) 11 cycles	59
Figure 4.7: XRD patterns of ZnO nanorods grown at ZnO seed layers annealed with different temperature.....	61
Figure 4.8: Top view of FESEM images of ZnO nanorods grown at ZnO seed layers annealed with different tempratures (a) 350°C, (b) 450°C, (c) 550°C and (d) 650°C	62
Figure 4.9: Side view of FESEM images of ZnO nanorods grown at ZnO seed layers annealed with different temperatures (a) 350°C, (b) 450°C, (c) 550°C and (d) 650°C	63
Figure 4.10: Reflectance test of ZnO nanorods on Si substrate.....	64
Figure 4.11: Wetting contact angle of water on bare Si substrate.....	65
Figure 4.12: Wetting contact angle of Si substrate covered with highly coverage of ZnO nanorods.....	66
Figure 4.13: Schematic diagram of the growth of ZnO nanorods on bare Si substrate	68

Figure 4.14: FESEM image of ZnO nanorods grown on bare Si substrate.....68

Figure 4.15: Schematic diagram of the growth of ZnO nanorods on ZnO seed layer pre-deposited on Si substrate.....69

Figure 4.16: FESEM image of ZNO nanorods grown on highly (002) ZnO seed layer.....70

LIST OF TABLES

Table 2.1: Lattice parameter (a_0), interatomic distance (d_0), and mismatch factor ($\Delta d/d$) vs. ZnO for GaAs, InP, GaN and 4H-SiC (Faugier-tovar <i>et al.</i> , 2016).....	29
Table 3.1: Raw materials and chemicals that were used in synthesizing of ZnO seed layer and ZnO nanorods on Si substrates via solution precipitation method.....	39
Table 3.2: Conditions of ZnO seed layer at different rpm.....	44
Table 3.3: Deposition conditions of ZnO seed layer coating cycles on the Si substrate.....	44
Table 3.4: Annealing temperature of ZnO seed layer.....	45
Table 4.1: Percentages of surface coverage on Si substrate prepared at different rotational speed.....	56
Table 4.2: Percentages of surface coverage on Si substrate at different number of coating cycles.....	60
Table 4.3: Percentages of surface coverage on Si substrate at different annealing temperatures.....	63

LIST OF ABBREVIATIONS

ALD	Atomic layer deposition
CBD	Chemical bath deposition
CVD	Chemical vapor deposition
FESEM	Field Effect Scanning Electron Microscopy
FET	Field effect transistor
FWHM	Full width half maximum
GaAs	Gallium Arsenite
HCl	Hydrochloric acid
HCP	Hexagonal closed packed
HMTA	Hexamethylenetetramine
HNO ₃	Nitric acid
HRTEM	High Resolution Transmission Electron Microscopy
i.e.	In other words
ICDD	International Centre of Diffraction Data
In	Indium
LED	Light emitting diode
NH ₃	Ammonia
pH	Potential of hydrogen
PL	Photoluminescence

LIST OF SYMBOLS

$^{\circ}$	Degree
\AA	Armstrong
d_{hkl}	Interplanar spacing
e^{-}	Electrons
eV	Electron volt
g	Grams
h^{+}	Hole
hr	Hours
k	Rate constant
M	Molarity
mins	Minutes
ml	Mililitre
mM	milimolarity
n	Integer
OH	Hydroxyl radical
θ	Theta
λ	Lambda
μ	Micron

KESAN LAPISAN BIJIH ZINK OKSIDA KE ATAS PERTUMBUHAN ROD NANO ZINK OKSIDA MELALUI KAEDAH PEMENDAPAN LARUTAN

ABSTRAK

Terdapat pelbagai jenis substrat yang telah digunakan untuk pertumbuhan zink oksida di atas permukaan. Walau bagaimanapun, ianya sukar untuk mendapatkan rod nano zink oksida yang sangat sejajar di atas substrat kerana perbezaan substrat Si dan ZnO tidak sepadan. Masalah ini boleh ditangani dengan mendepositkan benih yang sangat (002) di atas permukaan substrat Si. Lapisan benih ZnO meningkatkan liputan dan selaras ZnO rod nano. Dalam projek ini, lapisan benih ZnO telah didepositkan pada substrat dengan menggunakan putaran salutan diikuti oleh penyepuhlindapan pos di udara. Precursor adalah zink dihidrat acetate larut dalam etanol. Pemendapan lapisan benih itu dilakukan pada kitaran yang berbeza lapisan dan pada kelajuan putaran yang berbeza (putaran setiap minit, rpm) untuk meningkatkan liputan rod nano ZnO. Imej-imej SEM menunjukkan bahawa jumlah tertinggi kitaran salutan (11 pusingan) dan rpm rendah (1000 rpm) mempunyai liputan rod nano ZnO yang terbaik di atas permukaan substrat. Untuk 1000 rpm, peratusan liputan rod nano ZnO pada permukaan adalah 82.2%, manakala bagi 1000 rpm padan 11 kitaran salutan adalah 84.42%. hasilnya menunjukkan bahawa kelajuan yang paling rendah dan jumlah tertinggi kitaran salutan memberi liputan lapisan benih ZnO yang terbaik. Seterusnya, rod nano ZnO telah disintesis daripada lapisan benih ZnO yang telah didepositkan melalui kaedah pemedapan larutan. Suhu penyepuhlindapan yang berbeza telah dijalankan pada lapisan benih ZnO untuk melihat perbezaan penjajaran. Rod nano ZnO yang bertumbuh pada suhu 350°C menunjukkan penjajaran menegak yang terbaik kerana rod nano telah berkembang pada paksi-c.

EFFECT OF ZnO SEED LAYER ON THE GROWTH OF ZnO NANORODS VIA SOLUTION PRECIPITATION METHOD

ABSTRACT

There are various types of substrates that have been used to grow ZnO nanorods on the surface. However, it is difficult to obtain highly aligned ZnO nanorods on Si substrate because of the large mismatches between ZnO and Si. This problem could be addressed by depositing a highly (002) oriented ZnO seed layer on the surface of Si substrate. The seed layer of ZnO improved the coverage and aligned growth of ZnO nanorods. In this project, ZnO seed layers were deposited on the Si substrate using spin coating followed by post annealing in air. The precursors were zinc acetate dihydrate dissolved in ethanol. The deposition of the seed layer was done at different cycles of coating and different rotational speed (rpm) to improve the coverage of ZnO nanorods. The SEM images shows that the highest number of coating cycles (11 cycles) and lowest rpm (1000 rpm) has the best ZnO nanorods surface coverage on the substrate. For 1000 rpm, the percentage of ZnO nanorods surface coverage is 82.2%, while for 1000rpm at 11 coating cycles was 84.42%. The result showed that the lowest speed and highest number of coating cycles provided the best coverage of ZnO seed layer. Next, ZnO nanorods were synthesized from the pre-deposited ZnO seed layer via solution precipitation method. Different annealing temperatures on the ZnO seed layer were conducted to observe the differences of the alignment. The ZnO nanorods grown at 350°C showed the best vertical alignment as the nanorods grew at *c*-axis.

CHAPTER 1

INTRODUCTION

1.1 Introduction

Nanoparticles are microscopic molecules with the size of less than 100 nm. Synthesis of nanoparticles with specified morphology is a territory of research because of a wide assortment of potential applications in biomedical, optical, and electronic fields (Agarwal, et al., 2017). These materials are adequately an extension between bulk materials and atomic or molecular structure. Zinc oxide (ZnO) is one of the materials that can be found in nano size. It is noted that ZnO nanoparticles could be synthesized via various techniques such as green synthesis (Agarwal, Venkat Kumar and Rajeshkumar, 2017), sol-gel (Hasnidawani *et al.*, 2016), hydrothermal (Saleh *et al.*, 2017), chemical vapour deposition (Meléndrez *et al.*, 2016), and laser pulse deposition (Guo *et al.*, 2008).

ZnO is a wide bandgap semiconductor (3.37 eV) with low exciton binding energy of 60 meV at room temperature (Shyu *et al.*, 2015). Thus, the conventional applications of ZnO are in sunscreen, paints, and coating as they are transparent to visible light and offer high UV absorption. In addition, ZnO displays antibacterial (Al-ogaidi, 2017), antifungal (Jamdagni, Khatri and Rana, 2016) and UV filtering (Sahoo, Biswas and Nayak, 2017) properties. Thus, these particles could be utilized as an element in antibacterial creams, balms and moisturizers, self-cleaning glass and cleanser. It is also reported that ZnO nanoparticles have been utilized as a part of food packaging material (Jamdagni, Khatri and Rana, 2016). Nevertheless, over the past decades, ZnO nanomaterials have attracted researchers attentions as potential materials for solar cells (Sathya *et al.*, 2012), gas sensors (Kumar *et al.*, 2015) , light emitting diodes (LEDs) (Choi *et al.*, 2010) and piezoelectric components (Sutradhar and Saha, 2015).

There are various synthesis methods that can be applied to grow ZnO nanorods via vapor route such as chemical vapor deposition (Meléndrez *et al.*, 2016), sputtering (Zhang *et al.*, 2015) and pulse laser deposition (Guo *et al.*, 2008). Yet these methods require severe synthesis conditions such as high vacuum (in the range of 3 to 20 mTorr) (Liu *et al.*, 2004), high synthesis temperature (500-1100°C) (Nguyen *et al.*, 2013) or foreign catalyst (Wu and Liu, 2002) for the growth of ZnO nanorods. In contrary, solution route such as sol-gel (Hasnidawani *et al.*, 2016), hydrothermal (Aneesh, Vanaja and Jayaraj, 2007), solution precipitation (Salahuddin, El-kemary and Ibrahim, 2015), offers relatively simple and cost effective approach. To synthesize ZnO nanorods in liquid solution, the effects of zinc salt, concentration of zinc salt, pH, growth temperature and growth time need to be controlled properly because the morphology of the ZnO nanorods is affected by these parameters (Song and Lim, 2007). The size of ZnO nanorods would decrease when the growth temperature decreases, while when the concentration of the zinc source increases, the length and diameter of ZnO nanorods also would increase. The length and diameter of ZnO nanorods are affected by growing time. ZnO nanorods with longer and larger diameter could be synthesized.

1.2 Problem statement

As shown in Figure 1.1, it is crucial to have a controlled morphology and alignment of ZnO nanorods for the fabrication of high performance field effect transistors (FETs) (Ahmad, Ahn and Hahn, 2017), LEDs (Choi *et al.*, 2010) and solar cells (Peng and Qi, 2011). Fabrication of these devices was achieved using vapour route such as CVD and was grown on substrates with small lattice mismatch (< 5%) with ZnO e.g. GaN (Wang *et al.*, 2005), sapphire (Jia *et al.*, 2013), and SiC (Sun *et al.*, 2008). The setup cost of CVD equipment is expensive and its operational cost is high as high temperature (500-1100°C) and vacuum pressure (3 to 20 mTorr Pa) are required. The cost for GaN and SiC

substrate of is expensive too. Therefore, although ZnO nanorods based opto-electronic devices demonstrated excellent performance, realization of these devices as commercial products is difficult attributed to the high fabrication cost. Figure 1.1 shows the SEM images of ZnO nanorods based on some applications.

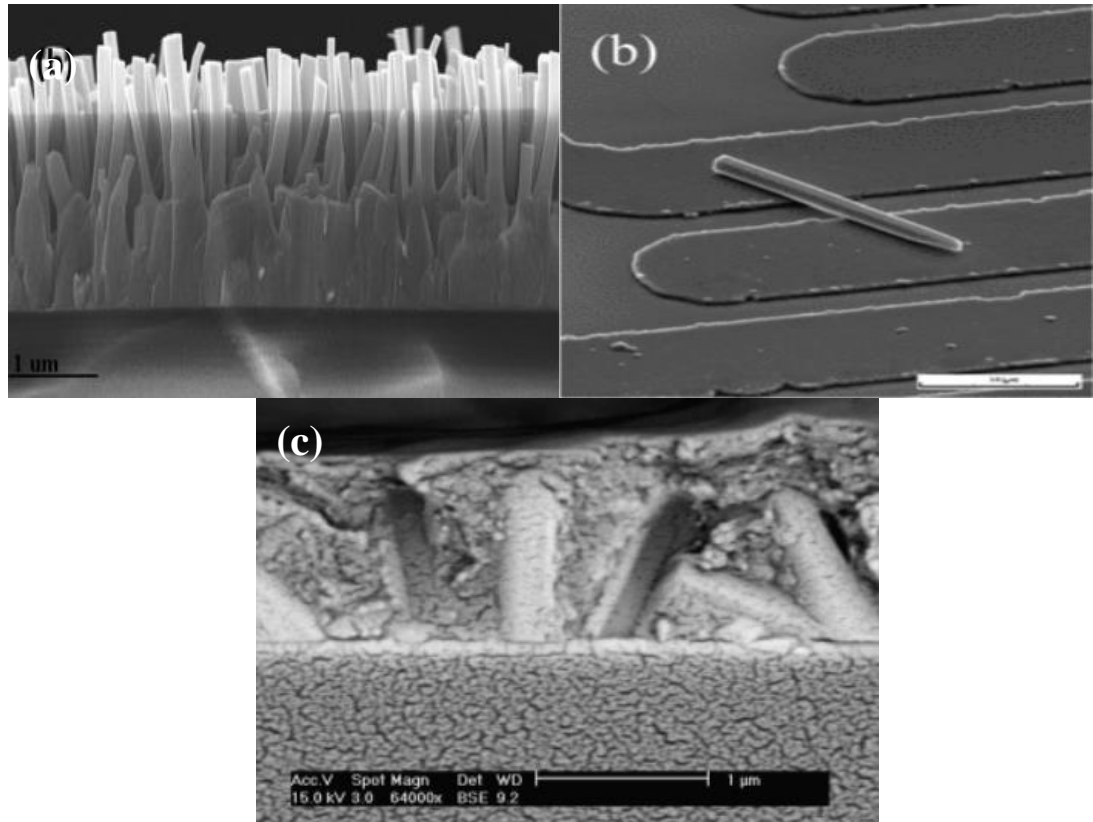


Figure 1.1: ZnO nanorods based (a)LED (Choi et al., 2010), (b) FET (Tsai et al., 2011) and (c) solar cell (Hames *et al.*, 2010).

In order to address the high fabrication cost issue, synthesis of ZnO nanorods on substrates via solution route e.g. sol-gel technique is an alternative approach. This method offers advantages such as simple synthesis process, no need of high synthesis temperature, pressure, energy and toxic chemical, and ability for process to be scaled up for large synthesis of nanoparticles. In fact, Ibupoto et al successfully grew random

growth ZnO nanorods on silicon substrate via sol-gel technique as shown in Fig. 1.2 (Ibupoto *et al.*, 2013)

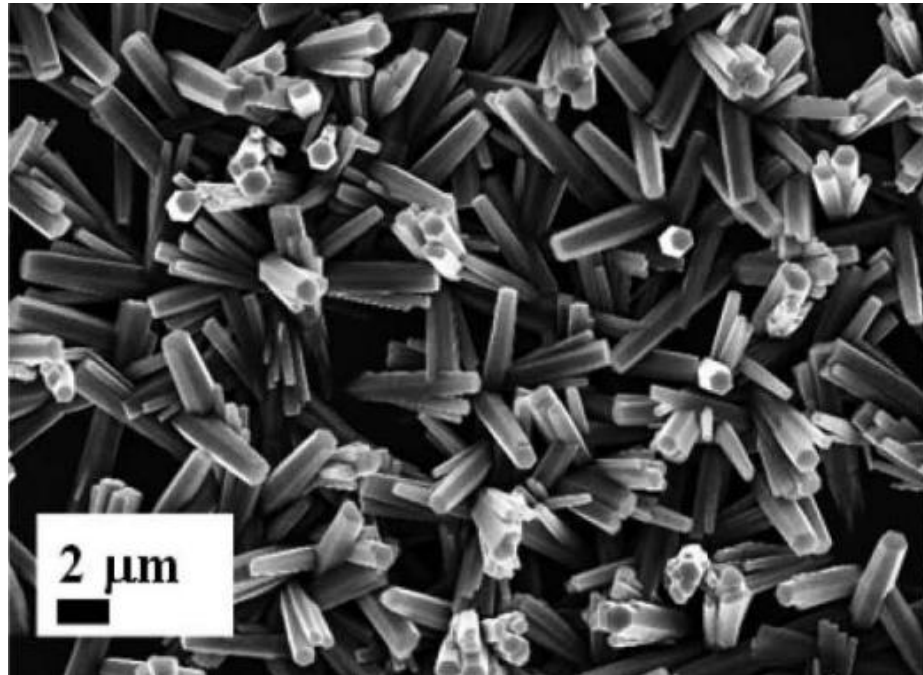


Figure 1.2: Randomly aligned ZnO nanorods grown on silicon substrate via sol-gel technique (Ibupoto *et al.*, 2013).

There are numerous types of substrates that can be used to grow ZnO nanorods such as silicon, polyethylene terephthalate, polystyrene and etc. Unfortunately, it is difficult to obtain highly aligned ZnO nanorods on these substrates because of the large mismatches (Rusli *et al.*, 2012). This problem could be addressed by depositing a highly (002) oriented ZnO seed layer on the surface of silicon substrate. The seed layer of ZnO improved the coverage and aligned growth of ZnO nanorods. The size of the nanoparticles on the substrate determines the size of the ZnO nanorods (Song and Lim, 2007). Nevertheless, highly (002) seed layer on silicon substrate normally obtained via the use of expensive equipment/technique such atomic layer deposition (Pung *et al.*, 2008) or

sputtering (Song and Lim, 2007), and microwave-assisted facile method (Ul Hassan Sarwar Rana, Kang and Kim, 2016).

In this project, effect of seed layer on the growth of ZnO nanorods on silicon substrate using solution precipitation method was systematically studied in order to address the problems of (i) high fabrication cost and (ii) randomly aligned growth of ZnO nanorods due to large lattice mismatch. Synthesis of ZnO nanorods on Si substrates via solution precipitation method is seldom developed by researchers. The coverage and alignment of ZnO nanorods on silicon substrate could be improved via pre-deposited of ZnO seed layer.

1.3 Research objectives

This project aims to synthesize a well-aligned and uniform coverage of ZnO nanorods using ZnO seed layer that deposited on silicon substrate via solution precipitation method. To achieve this goal, the following objectives are formed:

- I. To increase the coverage of ZnO nanorods on silicon substrate via deposition of seed layer.
- II. To improve the alignment of ZnO nanorods via highly (002) seed layer.

1.4 Project overview

This project has been divided into two parts. In the first part of the project, the (100) silicon (Si) substrates were cut into the size of 1 cm x 1 cm. The substrates were then cleaned with isopropanol for several times to remove contaminants on the surface. Next, ZnO seed layer was deposited onto the Si substrates. This was done by spin-coated the Si substrates with a mixture of zinc acetate dihydrate (0.2 M) with ethanol and

annealed at 350°C for 1 hour. The surface coverage of ZnO nanorods was optimized via systematic study on the (I) spin coater rotational speed (i.e. 1000, 2000, 2500 and 3000 rpm), (II) number of seed layer coating cycles (i.e. 3, 5, 7, 9 and 11 cycles). In addition, the growth alignment of ZnO nanorods was optimized via the annealing temperature of the ZnO seed layer i.e. 350°C, 450°C, 550°C and 650°C.

In the second part, the synthesis of ZnO nanorods via solution precipitation method was conducted by immersing the substrates into the mixture of zinc nitrate tetrahydrate, PVP and HMTA solution for 15 minutes. The solution was first stirred for 1 hour separately and then the mixture of zinc nitrate tetrahydrate and PVP were poured into HMTA solution drop by drop. Lastly, the samples were characterized by XRD and SEM to observe which parameters give the perfect aligned and uniform coverage of ZnO nanorods on silicon substrate. The overall project flow is illustrated in Figure 1.3.

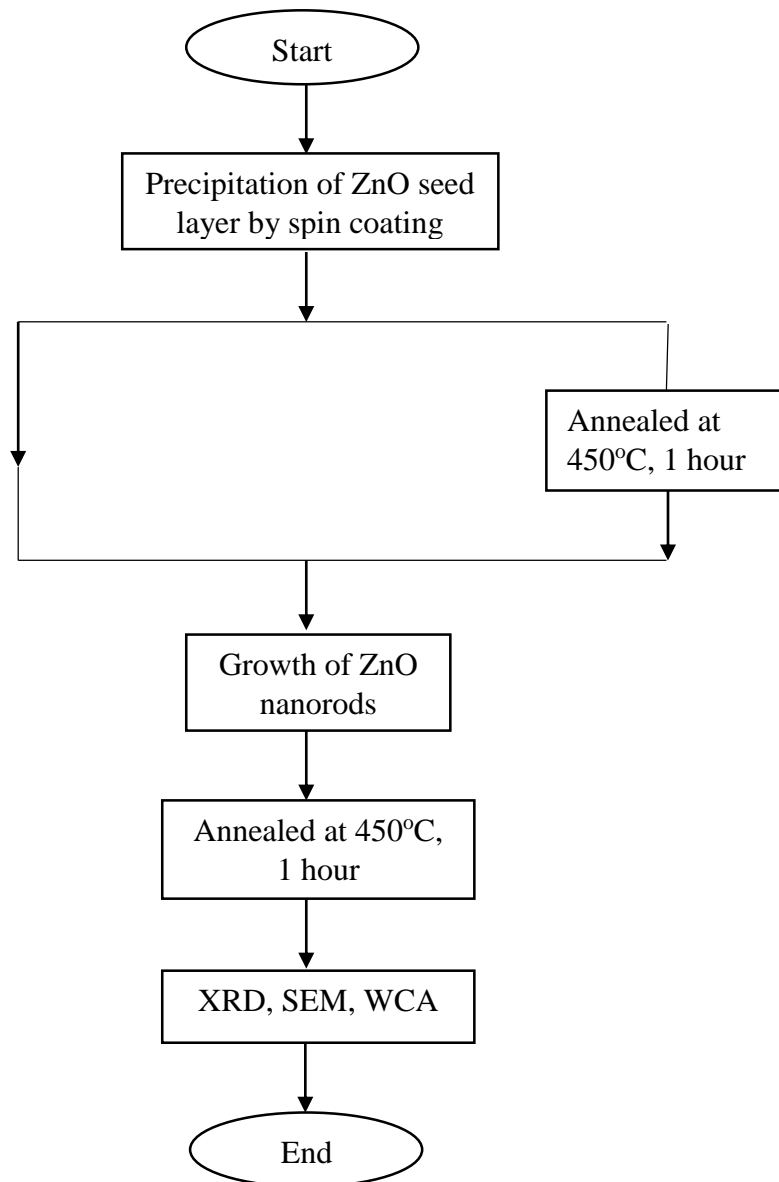


Figure 1.3: Process flow of synthesis and growth of ZnO nanorods on Si substrate.

1.5 Thesis outline

There are five chapters that compile in this thesis. First chapter describes the introduction, problem statement and research objectives of this project. Second chapter covers the background study of the effect of ZnO seeds on the growth of ZnO nanorods using solution precipitation method. While chapter three presents the materials and procedures used in synthesizing ZnO nanorods on the silicon substrate. This chapter also discusses the working principles and sample preparation of characterization techniques used in this project. Chapter 4 discusses the characterization results of ZnO seeds and the growth of ZnO nanorods on the silicon substrate. Lastly, chapter 5 concludes with key findings of this research work and suggestions for future works.

CHAPTER 2

LITERATURE REVIEW

2.0 History and background

Nanoparticles are microscopic molecules with the size of less than 100 nm. Recently, nanoparticles have been recognized for the development of new cutting-edge applications in communications, environmental protection, cosmetics and etc. The unique properties and utility of nanoparticles are arise from a variety of attributes, including similar size of nanoparticles and biomolecules such as proteins and polynucleic acids (Vaseem, Umar and Hahn, 2010). However, metal oxide nanoparticles stand out as one of the most flexible materials, due to their unique properties and functionalities. ZnO is one of the metal oxides that can be found in nano size. These nanoparticles display antibacterial (Al-logaidi, 2017), antifungal (Jamdagni, Khatri and Rana, 2016) and UV filtering (Sahoo, Biswas and Nayak, 2017) properties.

2.1 ZnO properties

Zinc oxide is an inorganic compound with the formula of ZnO. It is a white powder that is insoluble in water. ZnO is present in the earth's crust as the mineral zincite. It is a wide bandgap semiconductor (3.37 eV) belongs to the semiconductor groups of II-VI semiconductor. It is an n- type semiconductor as the majority charge carriers are electrons which contributed from the defects such as zinc interstitials and oxygen vacancies. Because of large exciton binding energy of 60 meV at room temperature, it has potential applications in optoelectronics, piezoelectronic and photocatalyst applications (Sutradhar and Saha, 2015). Also, it one of the best photocatalysts because of its low cost, nontoxic nature and photogenerated holes with high oxidizing power that suitable for the degradation of environmental pollutants (Chou *et al.*, 2017).

ZnO has a wurtzite crystal structure with lattice parameters $a = 0.3296$ nm and $c = 0.5265$ nm. It belongs to the space group of $C6m$ (Naveed Ul Haq *et al.*, 2017). Figure 2.1 shows the crystal structure of ZnO. It consists of two interpenetrating hexagonal closed packed (HCP) sub-lattices, which each composes of either Zn or O atoms (Vaseem, Umar and Hahn, 2010). Each of Zn ions are surrounded by of O ions tetrahedrally and vice versa. The most common face terminations of wurtzite ZnO are the polar Zn terminated (0001) and O terminated ($\bar{0}001$) faces. These polar faces are known to have different chemical and physical properties. In fact, the O terminated face possesses a slightly different electronic structure compared to Zn terminated face. As each ion is enclosed by four counter ions pointing towards corners of a tetrahedron, this tetrahedron configuration is accountable for the piezoelectricity and pyroelectricity of ZnO. This piezoelectricity of ZnO arises from its crystal structure and makes it valid for acoustic wave resonators and acoustic-optic modulators (Naveed Ul Haq *et al.*, 2017).

ZnO is one of the richest families of nanostructures among all the metal oxides. Some of the commonly found ZnO nanostructures such as nanocombs (Yang *et al.*, 2016), nanorings (Liu and Cai, 2008), nanobelts (Xi *et al.*, 2007), nanowires (Peng and Qi, 2011) and nanocages (Li *et al.*, 2016). The growth of these ZnO nanostructures were the result of tuning the growth rates along $\langle 2\bar{1}\bar{1}0 \rangle$ ($\pm [2\bar{1}\bar{1}0]$, $\pm [\bar{1}2\bar{1}0]$, $\pm [\bar{1}\bar{1}20]$); $\langle 01\bar{1}0 \rangle$ ($\pm [01\bar{1}0]$, $\pm [10\bar{1}0]$, $\pm [1\bar{1}00]$); and $\pm [0001]$.

In fact, $\pm [0001]$ is the fastest growth directions of ZnO. Thus ZnO nanorods/nanowires are widely seen in the synthesis process as shown in Figure 2.2 (a). Various ZnO nanostructures were produced by controlling the synthesis parameters, such as deposition temperatures (Gu *et al.*, 2015), pressures (Tao *et al.*, 2010), gas flux (Shabannia, 2015) and foreign catalysts e.g. Sn (Wang, 2004) and In (Tubtimtae and Lee, 2012).

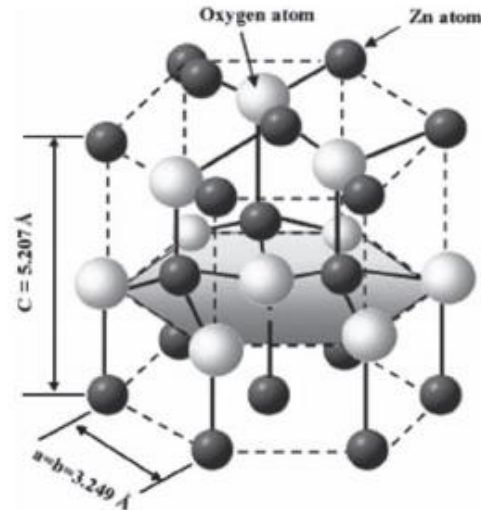


Figure 2.1: Hexagonal wurtzite structure model of ZnO (Vaseem, Umar and Hahn, 2010).

As shown in Figure 2.2 (b), ZnO nanobelts are usually grown by sublimation of ZnO powder without a catalyst. The nanobelt grows along $[0\ 1\ \bar{1}\ 0]$, with top and bottom flat surfaces $\pm (2\ \bar{1}\bar{1}\ 0)$ and side surfaces $\pm (0001)$ as illustrated in Figure 2.3. The growth of ZnO nanorings can be understood from the polar surfaces of nanobelts. The ZnO polar nanobelt, which is the building block of the nanoring, grows along $[1\ 0\ \bar{1}\ 0]$, with side surfaces $\pm (1\bar{2}\ 10)$ and top/bottom surface $\pm (0001)$ (Wang, 2004). It is found that the comb structure is an asymmetric growth along Zn- $[0001]$ (Liu and Cai, 2008). Lastly, by changing the composition of the source material, ZnO nanocages could be grown as shown in Figure 2.2(d). A mixture of commercial ZnO, SnO₂ and graphite powders in an atomic ratio of 2:1:1 was used as the source materials (Wang, 2004).

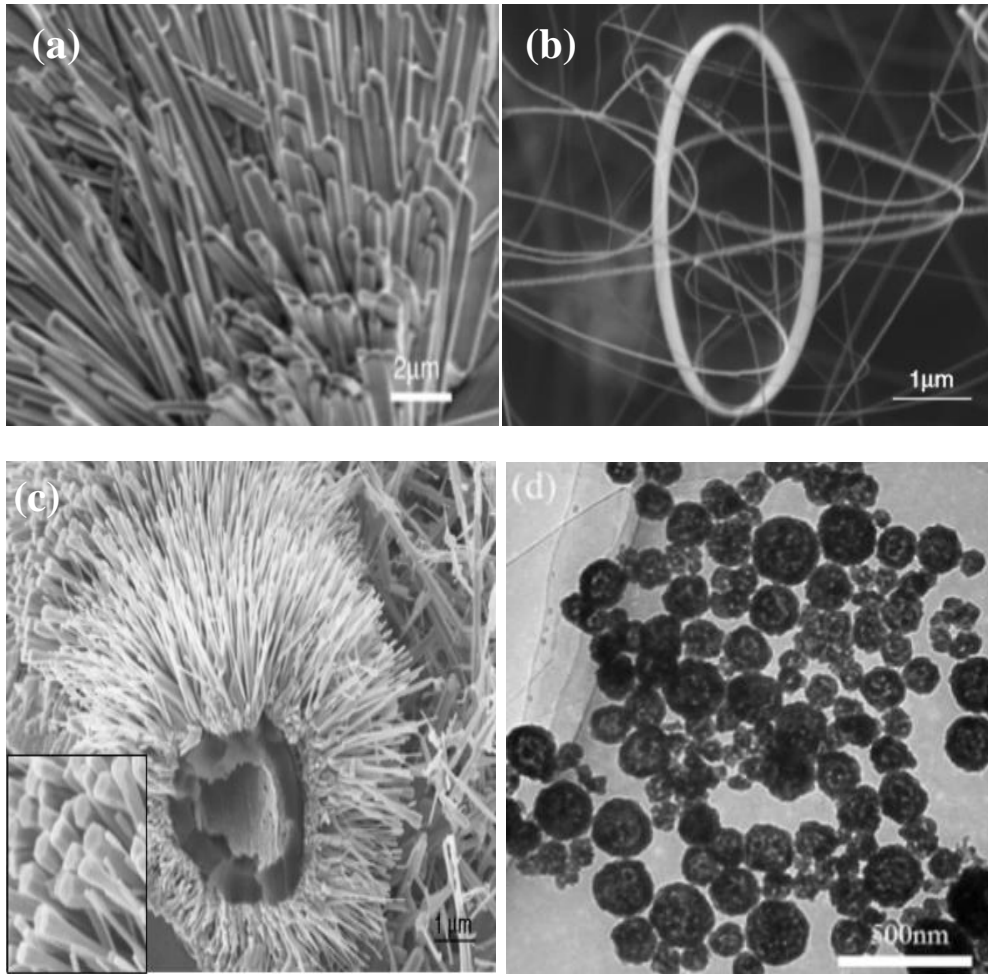


Figure 2.2: ZnO nanostructures (a) nanobelts, (b) nanorings, (c) nanowires and (d) nanocages (Wang, 2004).

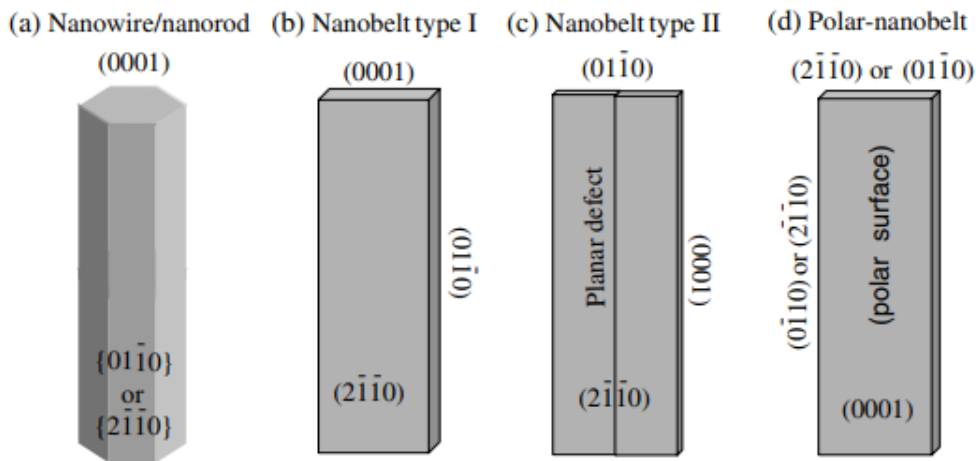


Figure 2.3: Growth morphologies of 1D ZnO nanostructures and corresponding facets (Wang, 2004).

2.2 Synthesis methods of ZnO nanostructures

There are various synthesis techniques to produce ZnO nanostructures. Generally, these synthesis techniques can be classified into vapor route and solution route. In vapor route, chemical vapor deposition (CVD) (Wu and Liu, 2002), physical vapor deposition (PVD) and atomic layer deposition (Huang *et al.*, 2013) techniques have been widely used to synthesize ZnO nanostructures. In vapor route, the condensed or powder source material is vaporized at elevating temperature and the resultant vapor phase condenses under certain conditions such as temperature, pressure, atmospheres and etc. In contrary, a wet chemical method has been proven to be a simple and versatile approach for synthesis of ZnO nanowires or nanorods due to its relatively low growth temperature and good potential for mass production (Xi *et al.*, 2007).

2.2.1 Solution routes

2.2.1.1 Sol-gel method

Sol-gel is one of the simplest methods to synthesize ZnO nanoparticles. It has the ability to control the particles size and morphology through systematic controlling of synthesis parameters. Sol-gel is a chemical solution process commonly used to make ceramic and glass materials in the form of thin films, fibers or powders (Harun *et al.*, 2016). A sol is a colloidal or molecular suspension of solid particles or ions in a solvent whereas a gel is a semi-rigid mass that forms when the solvent from the sol begins to evaporate and the particles or ions are left behind begin to combine together in a continuous network. The advantages of sol-gel method are (i) cheap and (ii) low temperature technique that allows for fine control on the product's chemical composition.

ZnO nanorods could be synthesized via sol-gel method. For instance, zinc acetate dehydrate ($\text{Zn}(\text{CH}_3\text{COO})_2 \cdot 2\text{H}_2\text{O}$) was used as a precursor and ethanol (CH_2COOH) as

solvent, while Sodium hydroxide (NaOH) and distilled water were used as medium (Hasnidawani *et al.*, 2016) to synthesize ZnO nanorods. The FESEM image of ZnO nanorods is demonstrated in Figure 2.4. The SEM image clearly shows high-density and randomly grown ZnO nanorods were successfully grown on the Si substrate (Kashif *et al.*, 2013).

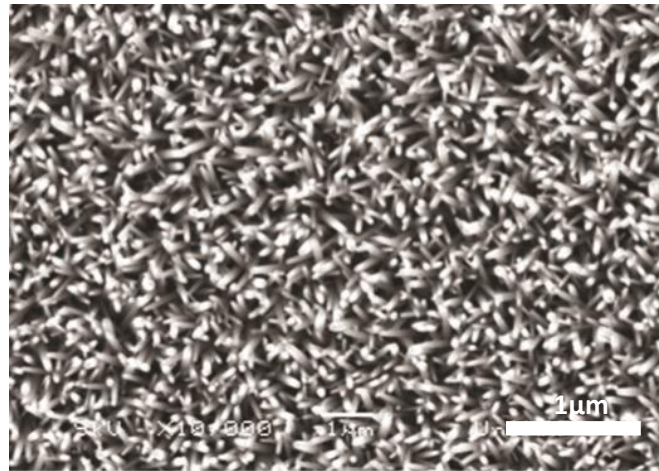


Figure 2.4: ZnO nanorods synthesized by sol-gel method (Kashif *et al.*, 2013).

2.2.1.2 Hydrothermal method

Hydrothermal method is also one of the methods to synthesize ZnO nanoparticles. Hydrothermal method requires autoclave apparatus for synthesis process. In general, it is conducted in an enclosed system at a high autogeneous pressure. The required temperature for preparing powder can be greatly reduced because of enhanced reactivity of reactive species, and fine particles with high sinter-ability is the benefit of the closed system with pressure. In addition, the evaporation of volatile species can be suppressed, and the stoichiometric of ceramics can be maintained. The particles properties such as morphology and size can be controlled via hydrothermal process by altering the reaction temperature, time and concentration of the precursors. As compared to sol-gel method, the crystal quality and particle size could be controlled relatively easy. It also offers

advantages such as catalyst-free growth and large area uniform production (Aneesh, Vanaja and Jayaraj, 2007).

Figure 2.5 shows the FESEM image of ZnO nanorods synthesized via hydrothermal method. The average diameter of ZnO nanorods gradually increased from 64 nm to 80 nm with increasing heat treatment temperature of the seed layer. The ZnO crystal structure consists of a number of alternating planes composed of coordinated Zn and O atoms along the *c*-axis direction (Ridhuan *et al.*, 2012).

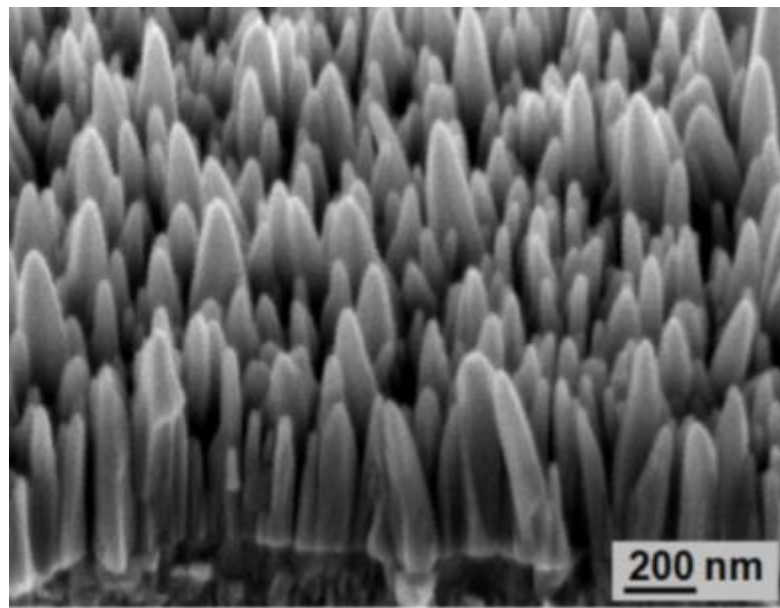


Figure 2.5: FESEM image of ZnO nanorods synthesized by hydrothermal method (Ridhuan *et al.*, 2012).

2.2.1.3 Solution Precipitation method

The simplest method used for synthesizing ZnO nanoparticles is by precipitation method. Precipitation method is a low-temperature, cost effective and scalable process. It has been used for preparing a wide variety of ZnO nanostructures (Salahuddin, El-kemary and Ibrahim, 2015). This method used different precursors such as Zinc nitrate tetrahydrate ($\text{Zn}(\text{NO}_3)_2 \cdot 4\text{H}_2\text{O}$), polyvinyl pyrrolidone (PVP), and 1,3-hexamethylenetetramine (HMTA, $\text{C}_6\text{H}_{12}\text{N}_4$) for the growth of ZnO nanorods.

Figure 2.5 shows ZnO nanoparticles that were prepared using precipitation method. The ZnO particles aggregated after washing and drying at the end of synthesis process. Meanwhile, Figure 2.6 shows the room temperature photoluminescence (PL) spectra of the ZnO nanoparticles heat treated at different annealing temperatures. All of the PL spectra possessed one obvious intrinsic UV emission peak in the range of 378.50-379.80 nm, which corresponds to the exciton recombination related to the near-band edge emission (Salahuddin, El-kemary and Ibrahim, 2015).

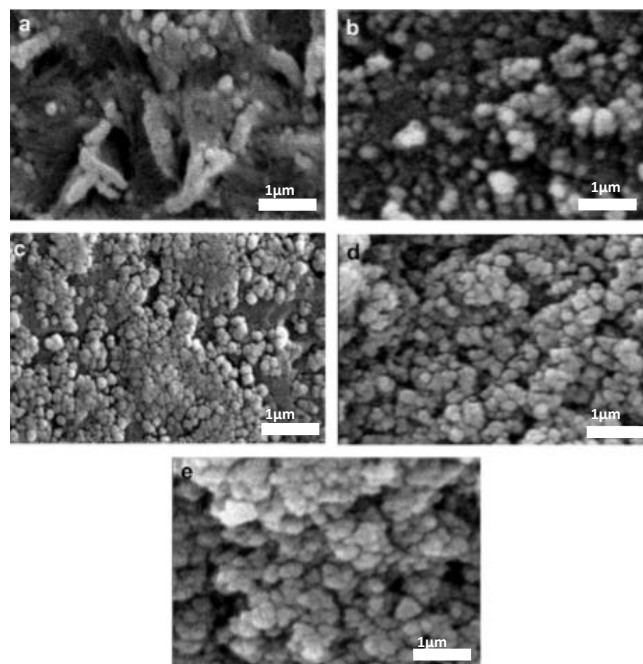


Figure 2.6: FESEM micrographs of ZnO nanoparticles synthesized by solution precipitation method and synthesized at different annealing temperatures (a) as-obtained precursor, (b) 250°C, (c) 350°C, (d) 450°C and (e) 550°C (Raoufi, 2013).

2.2.1.4 Factors that affect ZnO nanorods growth using solution route

I. Effect of precursor stirring

In order to get a proper substitution in solid solution, a thorough mixing of individual synthesis precursor solutions is an important factor that need to be considered. Thus, solution-based methods commonly require low temperature and are very effective in producing high quality nanocrystalline samples. The stirring of precursor solutions in preparation steps is required for enhancing the chemical homogeneity of the ionic species and hence increase the rate of synthesis by lowering the influence of the activation energy during the synthesis process. The control of the rate of hydrolysis of the hexamethylenetetramine (OH^- concentration) in the preparation step by varying the stirring durations of the precursor solutions affected the ZnO nanorods (Alnoor *et al.*, 2015).

Figure 2.7 shows the SEM image of ZnO nanorods by varying stirring durations of precursor solutions. The SEM images show vertically aligned hexagonal shaped ZnO nanorods. However, as the stirring durations increased, the diameter of nanorods were increased from 120 nm for 1 hr to 180 nm and 300 nm for 3 and 5 hrs of stirring durations respectively. Upon increasing the stirring duration up to 15 hrs, the nanorods diameters decreased to 200 nm. These show that the increase and decrease of the diameter of ZnO nanorods were affected by stirring durations attributed to the super saturations state of OH^- and Zn^{2+} species (Alnoor *et al.*, 2015).

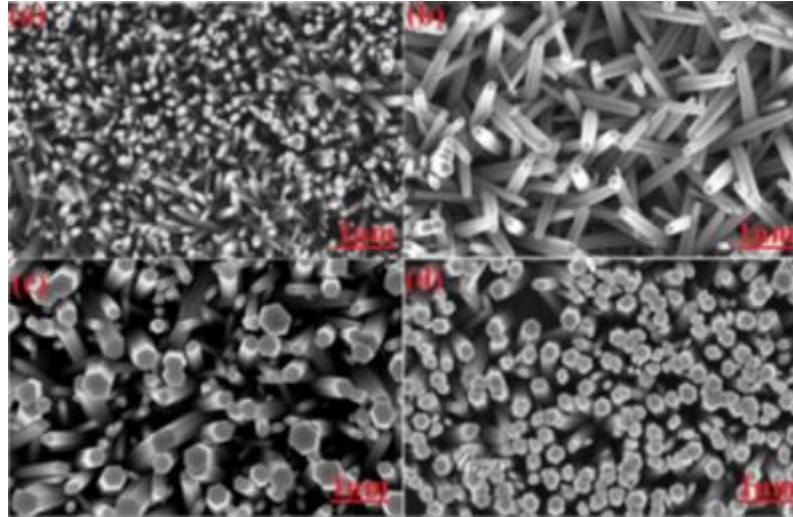


Figure 2.7: FESEM image of ZnO nanorods by varying stirring solutions (a) 1hr, (b) 3hrs, (c) 5hrs and (d) 15hrs respectively (Alnoor et al., 2015).

II. Effect of precursor concentration

The precursor concentration has a significant influence on the morphology and crystal structure and crystal size of ZnO nanorods. Figure 2.8 shows the FESEM image of synthesized ZnO nanorods at different precursor concentrations from 1 mM up to 9 mM. Generally, ZnO nanorods synthesized at different precursor concentration were hexagonal shape. By increasing the precursor concentration while keeping the deposition time (6hrs) and deposition temperature at (90°C) fixed, the shape and density of ZnO nanorods were changed. At lower concentrations (1 mM to 3 mM), round shape nanorods were observed, which suggests that the growth mechanism did not favour the forming of nanorod morphology under these conditions. A prismatic shaped ZnO nanorod was basically a well-ordered crystal with visible {10-10} planes.

By increasing the precursor concentration, high quality hexagonal ZnO nanorods were observed. The increase in density of ZnO nanorods could be recognized as a result

of enhanced Zn^{2+} and OH^{2-} species due to increase in concentration. Besides, the diameter of ZnO nanorods increased with the precursor concentration (Mustafa *et al.*, 2017).

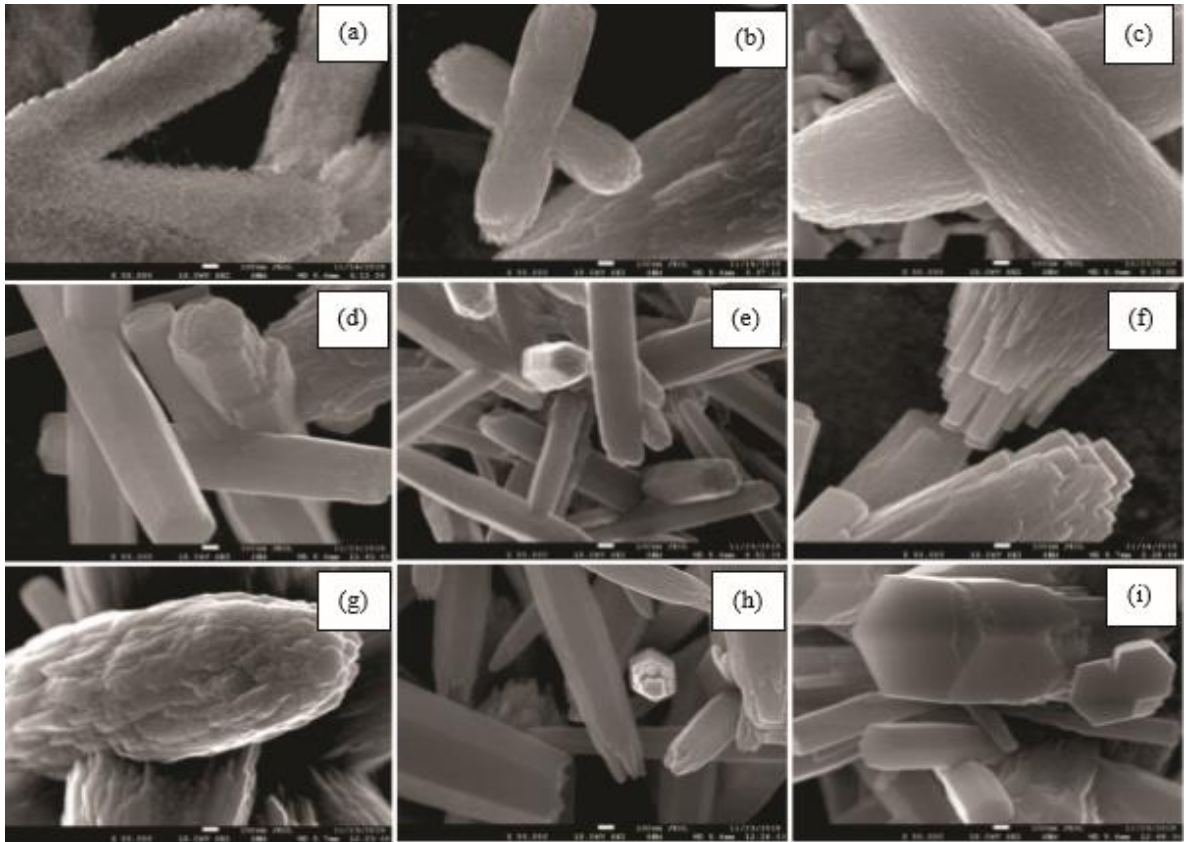


Figure 2.8: FESEM images of ZnO nanorods synthesized at different precursor concentrations (1 mM to 9 mM) respectively (Mustafa *et al.*, 2017).

III. Effect of pH

pH also plays an important role on the growth of ZnO nanorods. It has been reported that the pH on the hydrothermal growth of the ZnO nanorods is crucial because of hydrogen ions (OH^-) are strongly related to the reactions that produce the ZnO nanorods. Figure 2.9 shows the SEM images of various nanostructures grown under different pH values. Figure 2.9 (a) and 2.9 (b) display SEM images for the initial pH of 1.8 and 4.6, respectively. The ZnO structures were nanorods with hexagonal shape. The ZnO diameter and length increased with addition of HNO_3 or HCl or by lowering the pH values. In brief, very large dimension rods were obtained at $\text{pH} < 4.6$ (Amin *et al.*, 2011). Figure 2.9 (c) shows high density nanostructures prepared from solutions at $\text{pH}_{\text{initial}} = 6.6$

without adding of NH_3 . When the pH was increased to 8, ZnO nanotetrapods were obtained as shown in Figure 2.9 (d). This can be attributed to the hydroxide concentrations increased in the solution, giving rise to the anisotropic growth directions. When the pH increased to 9.1, the growth rate increased due to the increases of OH^- concentration which produced ZnO particles in the solution. The resulting structure (Fig. 2.9 (e)) was a flower like structure with thick arms while Fig. 2.9 (f) shows ZnO urchin-like structures with needles length of 2 μm and a diameter of ~ 50 nm for samples prepared from a solution with pH = 11.2. So, it can be concluded that the increases in pH and addition of acids will change the structures of ZnO nanostructures.

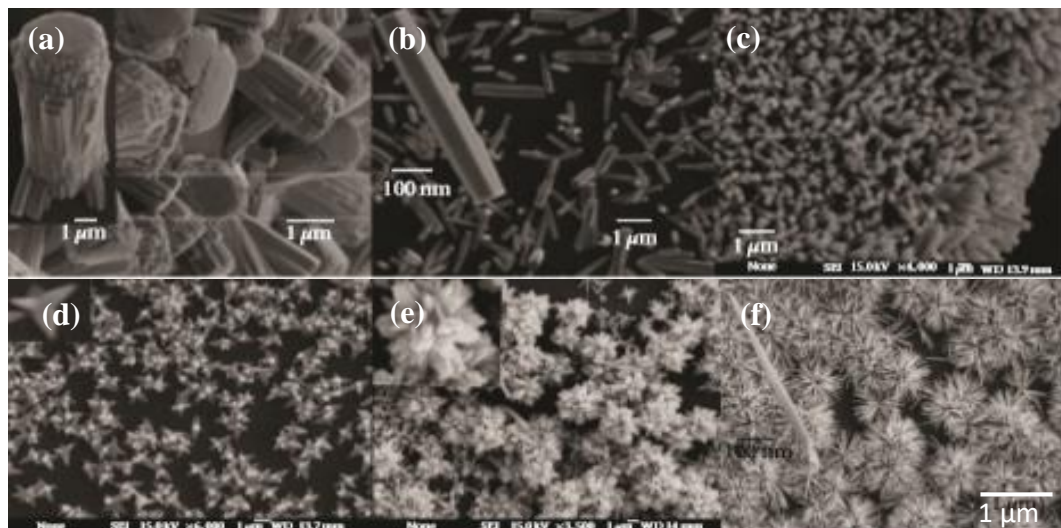


Figure 2.9: SEM images of ZnO nanostructures on Si substrates grown with different aqueous solutions at (a) pH value of 1.8, (b) pH value of 4.6, (c) pH value of 6.6, (d) pH value of 9.1, (e) pH value of 10.8, (f) pH value of 11.2 (Amin et al., 2011).

IV. Effect of growth time

In addition, time is also one of the factors that will affect the size of ZnO nanorods. Time is largely influencing the length and diameter of ZnO nanorods. A longer the synthesis time leads to a longer and larger diameter of ZnO nanorods. Figure 2.10 shows the cross-sectional SEM images of ZnO nanorods grown at different durations. Figure

2.10 (a) shows ZnO nanorods grown for 1 hour, with an average length of 500 nm, indicating that rods are emerging on the nucleation sites. These nanorods continued to grow with increasing of growth duration. When the growth was conducted for 3 hours, the average length of nanorods obtained is 1.0 μm (Fig. 2.10 (b)). By increasing the growth time to 6 hrs, the nanorods length was up to 1.8 μm as shown in Figure 2.10 (c). The length has increased up to 2.2 μm when the growth time was increased to 10 hrs as seen in Figure 2.10 (d), while no further increase of ZnO nanorods size was observed above 10 hrs. The inset in Figure 2.10 shows a top view of the corresponding SEM images, which the diameter of ZnO nanorods were changed from 150 nm to 500 nm with the change of time as stated above. In summary, the growth duration controls the size of the final ZnO structure (Amin *et al.*, 2011).

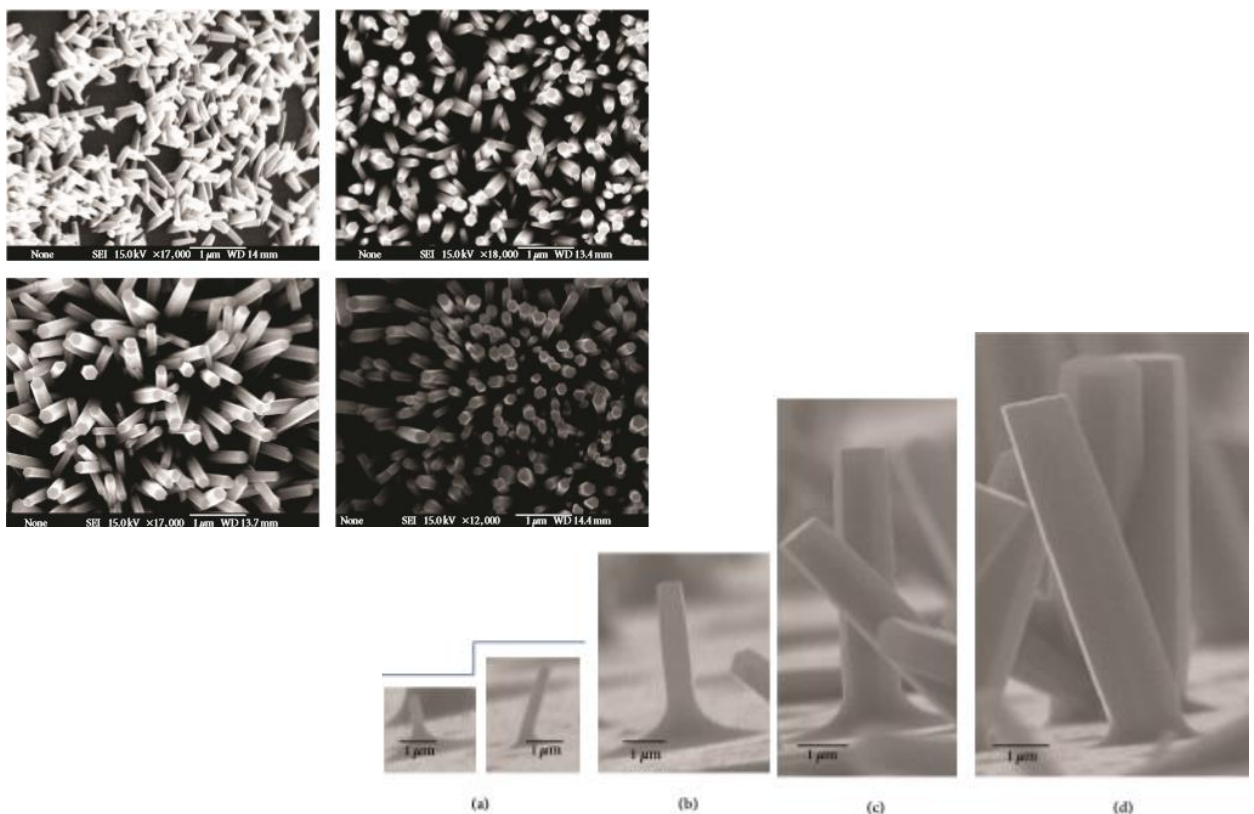


Figure 2.10: Cross-sectional SEM images of ZnO nanorods at different growth times; (a) 1hr, (b) 3 hrs, (c) 6 hrs, and (d) 10 hrs. The inset shows the corresponding top view of SEM images (Amin *et al.*, 2011).

2.2.2 Vapor routes

2.2.2.1 Chemical Vapor Deposition (CVD) method

Chemical vapor deposition method uses relative high synthesis temperatures to produce arrays of ZnO nanorods on a silicon substrate using (Guan and Pedraza, 2008). CVD involves flowing of a carrier gas or precursor gases into a chamber containing one or more heated objects to be coated. For example the precursor gases used were Ar (carrier gas) and O₂ (one of the precursor gas) with different concentrations ratio (Kim, Kim and Kim, 2017). Chemical reactions occur on and near the hot surfaces, causing deposition of thin film/nanostructures on the surfaces. This is accompanied by the production of chemical by-products that are exhausted out of the chamber along with unreacted precursor gases (Creighton and Ho, 2001). For instance, zinc acetylacetonate hydrate (Zn(C₅H₇O₂)₂.xH₂O) was evaporated in order to grow the ZnO nanorods on fused silica substrate. Ar was used as a carrier gas and the mass flow controllers were separately controlled the flow of Ar and O₂ gases (Kim, Kim and Kim, 2017). Figure 2.11 shows the schematic diagram of the CVD system.

The densely populated nanorods arranged vertically on the substrate, and had typical lengths up to tens of microns in low magnification SEM image were shown in Figure 2.12 (a). While for high magnification of SEM images (Figure 2.12 (b)) of ZnO confirmed that the nanorods were straight and smooth with fairly uniform diameter and length (Wang *et al.*, 2004). Figure 2.12 (c) is a top view of the nanorods, where the hexagonal cross-section feature of each rod was observed.

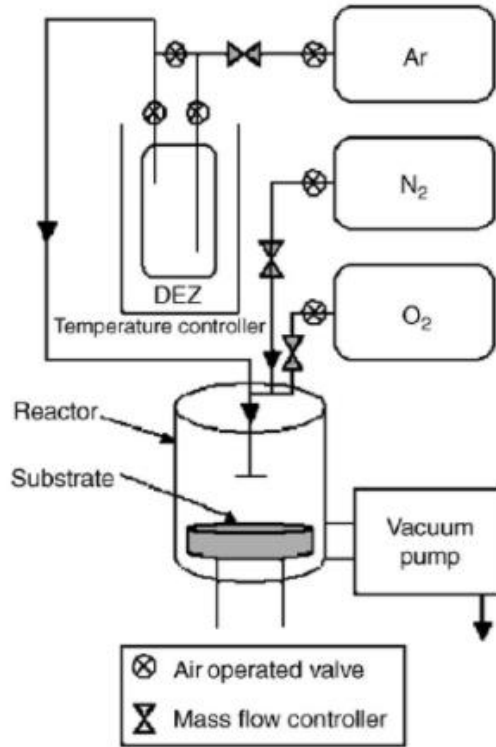


Figure 2.11: Schematic diagram of CVD process (Kim, Kim and Kim, 2017).

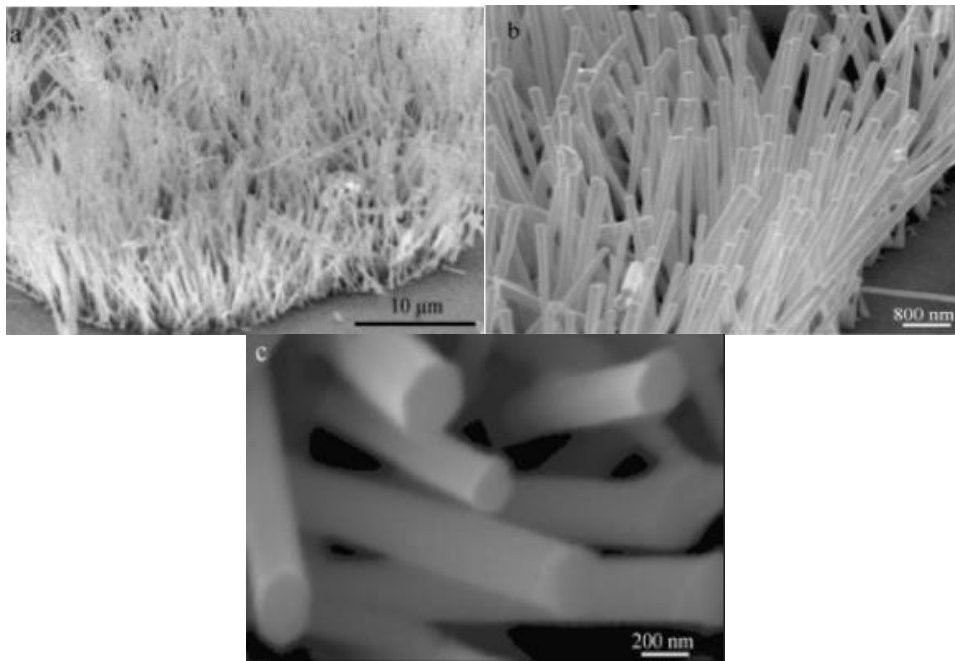


Figure 2.12: ZnO nanorods synthesized by CVD method, (a) low magnification SEM image, (b) high magnification SEM image, and (c) top view of SEM image (Wang et al., 2004).

Figure 2.13 shows the photoluminescence (PL) emission spectra of ZnO nanoparticles produced by CVD and post-annealed at different temperature. As can be seen from the figure below, all of the PL spectra of the products possess one obvious intrinsic UV emission peak in the range of 378.5-379.8nm, which corresponds to the exciton recombination related to the near band edge emission. Obviously, the intensity of UV emission peak increased as the annealing temperature increases from 250 to 550°C. This indicates that the crystalline nature of the samples were improved. The spectrum of the product (d), annealed at 550°C exhibits the strongest PL peak (94 Int. %) at 378.5nm, while product (a) annealed at 250°C has a PL peak (50 Int. %) at 379.8nm. Both of these peaks values are close to the theoretical energy band-gap of ZnO (Raoufi, 2013).

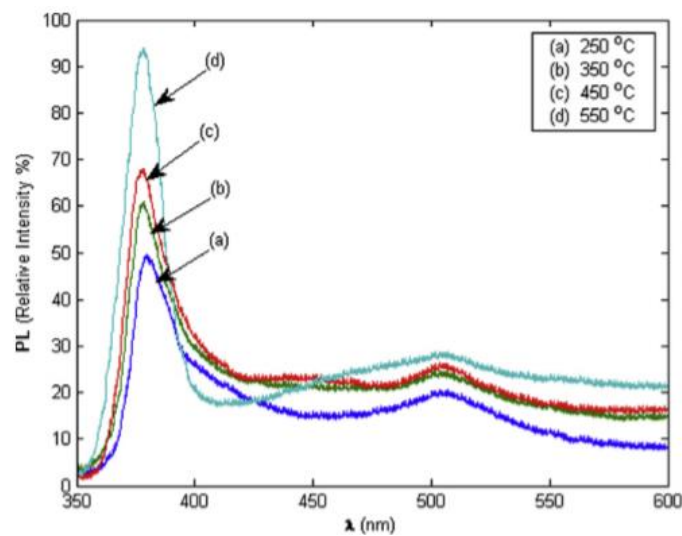


Figure 2.13: Room temperature photoluminescence (PL) emission spectra for ZnO nanoparticles at different annealing temperatures (Raoufi, 2013).